Robust Image Watermarking Based on Psychovisual Threshold

Ferda Ernawan

Faculty of Computer Systems and Software Engineering, Universiti Malaysia Pahang, Lebuhraya Tun Razak 26300 Gambang Kuantan, Pahang, Malaysia
E-mail: ferda@ump.edu.my

Abstract. Because of the facility of accessing and sharing digital images through the internet, digital images are often copied, edited and reused. Digital image watermarking is an approach to protect and manage digital images as intellectual property. The embedding of a natural watermark based on the properties of the human eye can be utilized to effectively hide a watermark image. This paper proposes a watermark embedding scheme based on the psychovisual threshold and edge entropy. The sensitivity of minor changes in DCT coefficients against JPEG quantization tables was investigated. A watermark embedding scheme was designed that offers good resistance against JPEG image compression. The proposed scheme was tested under different types of attacks. The experimental results indicated that the proposed scheme can achieve high imperceptibility and robustness against attacks. The watermark recovery process is also robust against attacks.

Keywords: *image watermarking; imperceptibility; modified entropy; psychovisual threshold; robustness; watermark embedding; watermarking scheme.*

1 Introduction

Nowadays, multimedia data such as images are easily converted into digital content. The protection of intellectual properties in the form of digital images faces very serious challenges such as piracy, illegal redistribution, forgery and theft [1]. These challenges make digital image watermarking an important issue, as it protects against unauthorized duplication of digital images. Image watermarking means to embed a watermark without degrading the perceptual image quality and at the same time making it difficult to remove [2]. Image watermarking should be able to comply with imperceptibility, robustness and security. Embedding and extracting the watermark image should be limited to authorized users only.

In modern digital image watermarking, the watermark insertion process exploits the characteristics of the human visual system (HVS). The watermark can be inserted in a redundant region of the HVS [3], especially in highly textured areas and significantly changing regions of an image or the image edges. The

Received February 20th, 2015, 1st Revision February 26th, 2016, 2nd Revision September 14th, 2016, Accepted for publication October 11th, 2016.
 ISSN: 2337-5787, DOI: 10.5614/itbj.ict.res.appl.2016.10.3.3

characteristics of the human visual system have previously been used in image watermarking applications [4,5]. Some image watermarking schemes were designed based on visual models of colour stimuli [6,7] or were derived from image compression to increase their robustness [8]. Embedding watermarks based on HVS properties is able to improve watermark robustness while still maintaining their imperceptibility. The watermark scheme in [9] utilizes the spatial masking principle of HVS to improve the watermark's strength. The HVS threshold has been utilized for improving the watermark's robustness for authentication [10] and protection [11].

In this paper, a specific location is proposed for embedding watermarks based on the psychovisual threshold. The contribution of the DCT coefficient to the reconstruction error was measured in natural and graphical images and analysed as an initial psychovisual threshold [12]. This threshold can be utilized to determine the location and strength of the watermark. In the proposed method, watermark embedding under the constraint of the psychovisual threshold was chosen in order for the watermark to be invisible to the human visual system and produces only imperceptible distortion. The entropy and edge entropy of each image block of the host image is considered to identify the region most suitable for watermark embedding. The watermark is inserted in a block with a minimum amount of edge entropy based on the psychovisual threshold. Watermark insertion based on the entropy of image pixels can improve the watermark's imperceptibility and robustness [13].

2 Psychovisual Threshold

A true-colour 24-bit image is converted to the YUV colour model. The advantage of the YUV colour model is that it separates chromatic and achromatic components. A YUV colour model consists of luminance Y, chrominance U and chrominance V, which have identical characteristics. The two-dimensional discrete cosine transform (DCT) is used to transform each component. The characteristics of DCT coefficients against reconstruction errors prescribe the psychovisual threshold for luminance and chrominance as shown in Figures 1 and 2 respectively. A green and a blue curve represent the average error reconstruction based on the minimum and maximum JPEG quantization values for each frequency order, respectively.

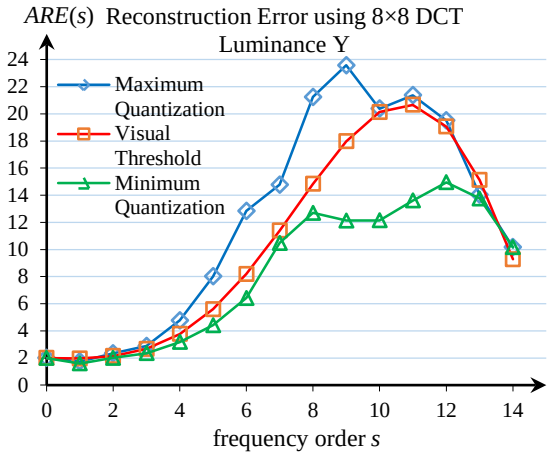

Figure 1 Average reconstruction for 40 real images error resulting from an increment of the DCT coefficient on the luminance.

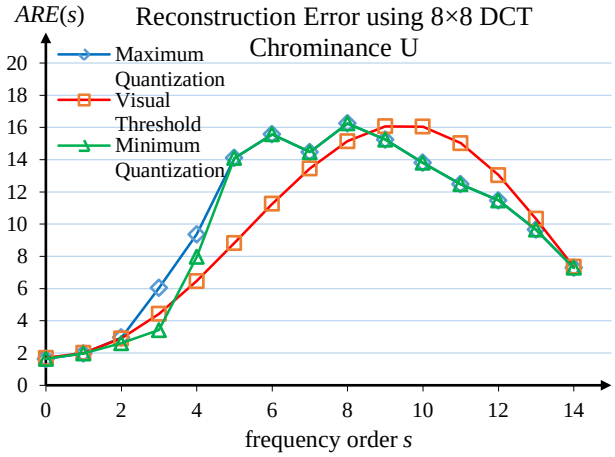

Figure 2 Average reconstruction error for 40 real images resulting from an increment of the DCT coefficient on the chrominance.

The average reconstruction error from an increment of the DCT coefficient on chrominance U is similar to the average reconstruction error on chrominance V. The sensitivity of the DCT coefficients on each frequency order against reconstruction errors produces an acceptable visual quality for the human visual system. The psychovisual threshold is set as a smooth transition curve of average error reconstruction as depicted by the red curve. According to Figures 1 and 2, the area under the psychovisual error threshold has potential resistance against JPEG quantization tables in image compression. In previous works, the psychovisual threshold has been applied to several image processing

applications, such as image compression [14-19], adaptive image compression [20,21] and image watermarking [12].

3 Embedding Location

The location of the embedding bits of a watermark in the low frequency order was chosen because it has more resistance against JPEG quantization tables in image compression. The loopholes of JPEG quantization tables are identified by differentiating between the average reconstruction error of the psychovisual threshold and the default 8×8 JPEG quantization tables. These gaps can be computed as follows in Eqs. (1) and (2):

$$Q_{GL} = Q_{VL} - Q_{CL} \tag{1}$$

$$Q_{GR} = Q_{VR} - Q_{CR} \tag{2}$$

The new quantization tables Q_{VL} and Q_{VR} for luminance and chrominance based on the psychovisual threshold are shown in Figure 3. The locations of loopholes $C_{5,1}$, $C_{4,2}$, $C_{3,3}$ luminance and $C_{3,2}$, $C_{2,2}$, $C_{2,3}$ chrominance in the JPEG quantization tables based on the psychovisual error threshold are indicated by the blackened cells:

16	14	13	15	19	28	37	55
14	13	15	19	28	37	55	64
13	15	19	28	37	55	64	83
15	19	28	37	55	64	83	103
19	28	37	55	64	83	103	117
28	37	55	64	83	103	117	117
37	55	64	83	103	117	117	111
55	64	83	103	117	117	111	90

18	18	23	34	45	61	71	92
18	23	34	45	61	71	92	92
23	34	45	61	71	92	92	104
34	45	61	71	92	92	104	115
45	61	71	92	92	104	115	119
61	71	92	92	104	115	119	112
71	92	92	104	115	119	112	106
92	92	104	115	119	112	106	100

Figure 3 Location of the embedded watermark within 8×8 DCT coefficients for luminance (left) and chrominance (right) of new quantization tables Q_{VL} and Q_{VR} based on the psychovisual threshold.

The watermark is expected to survive better in these locations against JPEG quantization tables Q_{CL} and Q_{CR} for luminance and chrominance, respectively. Watermark insertion in the blackened cell locations will not produce a significantly high quality degradation of the watermarked image. The entropy and edge entropy of the image pixels are employed to select the region block for watermark embedding. The entropy is used to measure the spatial correlation as defined by Eq. (3):

$$E = -\sum_{i=1}^{n} p_i \log_2(p_i) \tag{3}$$

where p_i denotes the occurrence probability of an event i with $0 \le p_i \le 1$ and $\sum_{i-1}^{n} p_i = 1$. Accordingly, the entropy together with the edge entropy of each block are considered to identify the block suitable for embedding. The edge entropy is defined as follows in Eq. (4):

$$E_{edge\_entropy} = \sum_{i=1}^{n} p_i \exp^{u_i} = \sum_{i=1}^{n} p_i \exp^{1-p_i} \tag{4}$$

where $u_i = 1 - p_i$ indicates the ignorance or uncertainty of the image pixels. The two measures of entropy of each block are then summed up and the values thus obtained are sorted in ascending order. The blocks with low entropy values are selected for watermark embedding until the number of selected blocks is equal to the watermark size.

Five true-colour images were selected as the host images to evaluate the watermarking scheme, i.e. “Baboon”, “Pepper”, “Boat”, “Airplane” and “Lena” [22]. The original high-fidelity images of size 512×512 pixels are shown in Figure 4.

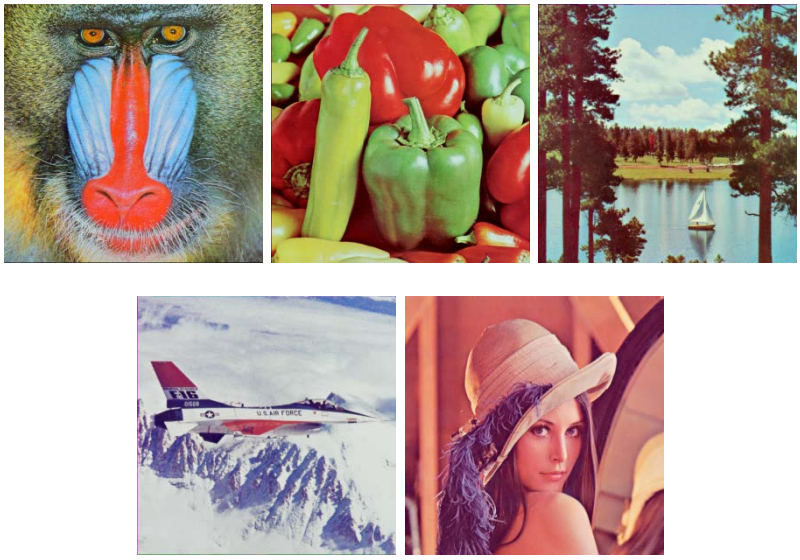

Figure 4 Original images “Baboon”, “Pepper”, “Boat”, “Airplane” and “Lena”.

4 Experimental Method

Embedding watermark schemes in a low frequency order will produce a higher quality degradation of the watermarked image. In 2002, Fridrich, *et al.* described how inserting bits of quantized DCT coefficients corresponding to medium frequencies provides a spare space to carry additional data against lossless image compression [23]. Embedding a watermark in a high frequency order makes the watermark less robust, with a higher probability of being lost if the watermarked image is compressed [24]. The watermark is inserted in the loopholes of the JPEG quantization tables because it has a complex texture area or edge in each block of the image. The human visual system is less sensitive to the edges of an image object [25]. The image watermarking scheme over edge entropy makes it possible to embed perceptually invisible watermarks and to make them more robust against attacks. A trade-off between robustness and imperceptibility is expected.

Figure 5 Original watermark image consisting of 25×75 pixels.

In this work, the Mersenne twister method was used to generate random numbers based on a secret key. The secret key was employed to encrypt and decrypt the watermark during insertion and extraction. The binary watermark *W* ("UMP") with a size of 25×75 pixels is shown in Figure 5.

4.1 Watermark Insertion

A host image is first divided into an 8×8 block image. Then the entropy and edge entropy are used to select the region block for watermark embedding. The suitable block is then transformed by the two-dimensional DCT and is embedded through random numbers in specific locations based on the psychovisual threshold. A random number selects the loophole positions in each 8×8 DCT block for inserting bits of the watermark. The watermark that is embedded in the host image is subjected to JPEG quantization values. The quantization value that is used in the embedding process is given as follows in Eq. (5):

$$\text{WQL} = \{18, 17, 16\} \text{ and } \text{WQCR} = \{21, 26, 26\} \tag{5}$$

The embedded watermarks for luminance are randomized by a private key, as given by (Eq. (6):

$$
\begin{aligned}
&C_{5,1} \quad \text{if } RNG(i,1)=0 \text{ and } RNG(i,2)=0 \text{ and } RNG(i,3)=0\\
&C_{4,2} \quad \text{if } RNG(i,1)=0 \text{ and } RNG(i,2)=0 \text{ and } RNG(i,3)=1\\
&C_{3,3} \quad \text{if } RNG(i,1)=0 \text{ and } RNG(i,2)=1 \text{ and } RNG(i,3)=0\\
&C_{5,1} \quad \text{if } RNG(i,1)=0 \text{ and } RNG(i,2)=1 \text{ and } RNG(i,3)=1\\
&C_{4,2} \quad \text{if } RNG(i,1)=1 \text{ and } RNG(i,2)=0 \text{ and } RNG(i,3)=0\\
&C_{5,1} \quad \text{if } RNG(i,1)=1 \text{ and } RNG(i,2)=0 \text{ and } RNG(i,3)=1\\
&C_{4,2} \quad \text{if } RNG(i,1)=0 \text{ and } RNG(i,2)=1 \text{ and } RNG(i,3)=0\\
&C_{3,3} \quad \text{if } RNG(i,1)=0 \text{ and } RNG(i,2)=1 \text{ and } RNG(i,3)=1
\end{aligned}
\tag{6}
$$

The embedded watermarks for chrominance are also randomized by a similar private key, as given by Eq.(7):

$$
\begin{aligned}
&C_{3,2} \quad \text{if } RNG(i,1)=0 \text{ and } RNG(i,2)=0 \text{ and } RNG(i,3)=0\\
&C_{2,2} \quad \text{if } RNG(i,1)=0 \text{ and } RNG(i,2)=0 \text{ and } RNG(i,3)=1\\
&C_{2,3} \quad \text{if } RNG(i,1)=0 \text{ and } RNG(i,2)=1 \text{ and } RNG(i,3)=0\\
&C_{3,2} \quad \text{if } RNG(i,1)=0 \text{ and } RNG(i,2)=1 \text{ and } RNG(i,3)=1\\
&C_{2,2} \quad \text{if } RNG(i,1)=1 \text{ and } RNG(i,2)=0 \text{ and } RNG(i,3)=0\\
&C_{3,2} \quad \text{if } RNG(i,1)=1 \text{ and } RNG(i,2)=0 \text{ and } RNG(i,3)=1\\
&C_{2,2} \quad \text{if } RNG(i,1)=0 \text{ and } RNG(i,2)=1 \text{ and } RNG(i,3)=0\\
&C_{2,3} \quad \text{if } RNG(i,1)=0 \text{ and } RNG(i,2)=1 \text{ and } RNG(i,3)=1
\end{aligned}
\tag{7}
$$

The calculation of the watermark quantity is given as follows in Eq. (8):

$$Q(i) = T \cdot W_Q \tag{8}$$

where the watermark weight to be embedded depends on threshold input T. Consider that when watermark $W = 1$, the watermark image is multiplied by "+1", whereas when watermark $W = 0$, it is multiplied by "−1" or subtracted from the host image.

The main steps of the embedding procedure can be described as follows:

Step 1: Take the host image block as input (block size is 8×8 pixels).
Step 2: Calculate the entropy and edge entropy of each image block to identify the block suitable for insertion. The two measures of entropy for each block are then summed up and the values thus obtained are sorted in ascending order. The block with the lowest value is selected for embedding until the number of selected blocks is equal to the watermark size.
Step 3: Transform the selected image block by the 2-D DCT.
Step 4: Generate a unique random number based on the secret key. The sequence value belongs to the set {0, 1}.

Step 5: Determine the selected location for watermark insertion based on a random number generator (RNG).
Step 6: Embed −1 or +1 into the selected location when the watermark value is 0 or 1 respectively.

The difference between the watermarked image and the original image was enhanced and shown in Figure 6.

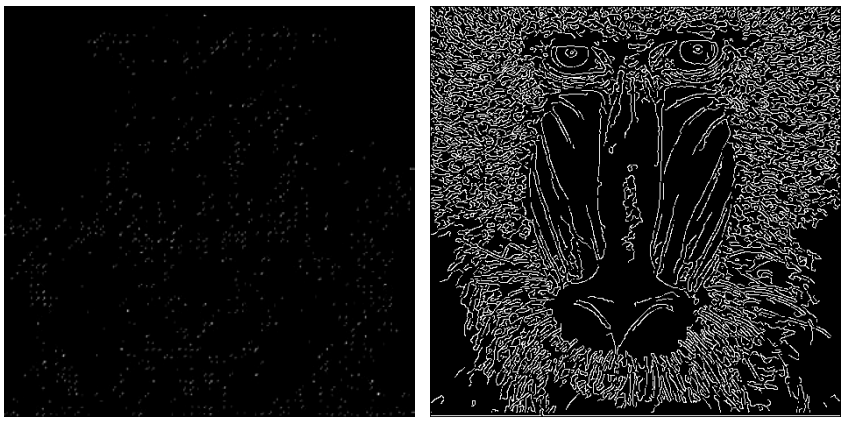

Figure 6 Enhanced embedding location based on the entropy of the "Baboon" image (left) and the edge entropy of the "Baboon" image (right).

4.2 Watermark Extraction

The watermark is extracted from the host image based on using the entropy and edge entropy to determine the selected block where the watermark is embedded. The watermark image is dispersed randomly on each selected block of the image based on the entropy and edge entropy. Extraction of the watermark involves a secret key to generate pseudo-random numbers. The watermark is detected by computing the correlation between the watermarked image and the watermark code.

The main steps of watermark extraction can be described as follows:

Step 1: Select the image blocks with low entropy values. The blocks with low entropy values are selected for extracting the watermark until the number of selected blocks is equal to the watermark size.
Step 2: Transform the image block by the 2-D DCT in the image block.
Step 3: Generate pseudo-random numbers with the same private key. These random numbers are used to find the location of the embedded watermark.

Step 4: Extract the watermark using an inner product algorithm. In order to extract the extracted sequence of the $X^*\{x^*(i), (1 < i < N)\}$, where $x^*(i) \geq 1$ means that the watermark is 1 and $x^*(i) \leq 0$ means that the watermark is 0.

A correlation coefficient is used to determine the watermark image. The correlation coefficient can be computed as follows in Eq. (9):

$$\rho = X \cdot X^* \tag{9}$$

where $X \cdot X^*$ is the inner product of X and the extracted sequence of X^*. If the correlation coefficient between watermarked image X and extracted sequence X^* is larger than a certain threshold, it is determined that the watermark exists.

4.3 Watermark Image Evaluation

The concealment of the watermark image was evaluated by peak signal to noise ratio (PSNR) and normalized cross-correlation (NC). The PSNR is defined as followsin Eq. (10) [26]:

$$PSNR = 10\log_{10}\left(\frac{255^2}{\sum_{i=0}^{M-1}\sum_{j=0}^{N-1}\sum_{k=0}^{2}\left\|g(i,j,k) - f(i,j,k)\right\|^2}\right) \tag{10}$$

where $g(i, j, k)$ represents the watermarked image, $f(i, j, k)$ represents the original host image, and k is the third index referring to the three RGB colors. PSNR is generally deployed for comparing imperceptibility performance [27]. The comparison between the recovered watermark and the original watermark was quantitatively analysed using the NC [28], which is defined as follows in Eq.(11):

$$NC = \frac{\sum_{i=1}^{K}\sum_{j=1}^{L} W(i,j).W'(i,j)}{\sqrt{\sum_{i=1}^{K}\sum_{j=1}^{L} W(i,j)^2 \sum_{i=1}^{K}\sum_{j=1}^{L} W'(i,j)^2}} \tag{11}$$

where $W(i, j)$ is the original watermark image and (i, j) is the recovered watermark image. $K \times L$ is the watermark image size and the value of NC is between 0 and 1. A higher value of NC means that the recovered watermark image is closer to the original watermark image.

5 Experimental Method

The watermarked images were tested with a number of attacks to evaluate the watermarking scheme's performance. The visual effects on the watermarked "Baboon" image and the corresponding extracted watermark under different types of attacks are shown in Figures 7 and 8, respectively. The extracted watermark image can be damaged but it can still be seen by the human eye.

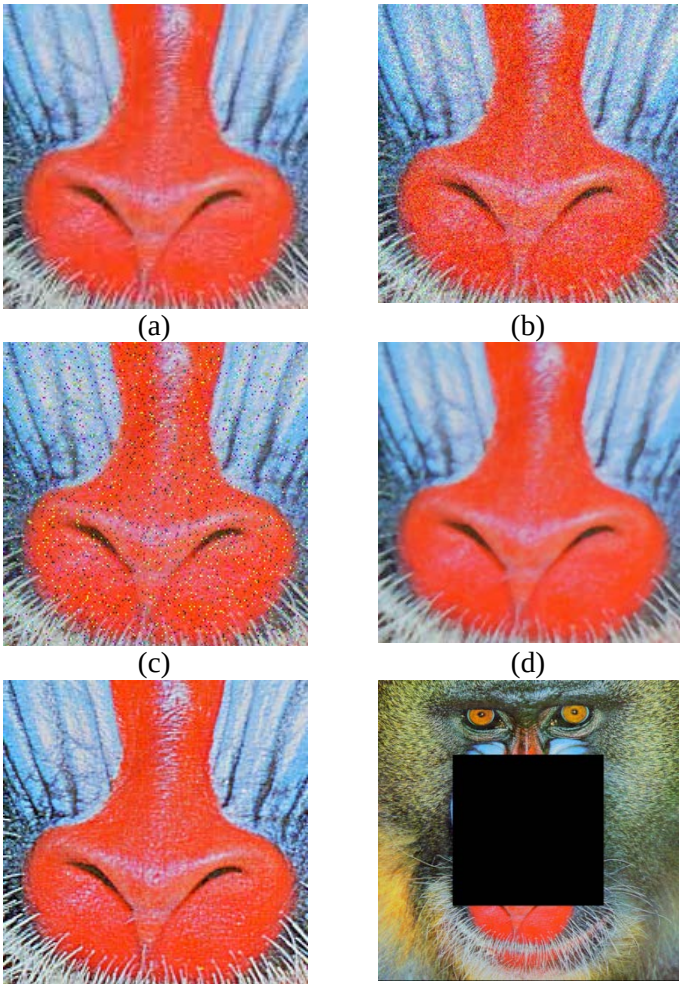

Figure 7 Attacked watermarked "Baboon" image: (a) JPEG compression, NC = 0.961; (b) Gaussian white noise 0.01, NC = 0.874; (c) salt and pepper noise 0.05, NC = 0.827; (d) median filter [3 3], NC = 0.944; (e) sharpening, NC = 0.991; and (f) cropping 25%, NC = 0.897.

Attacks	Baboon			
	***T* = 0.25**	***T* = 0.5**	***T* = 0.75**	***T* = 1**
No attack				
JPEG compression Q = 10				
JPEG compression Q = 30				
JPEG compression Q = 50				
JPEG compression Q = 70				
JPEG compression Q = 90				
Gaussian low pass filter [3 3]				
Gaussian noise 0.01				
Salt and pepper noise 0.05				
Median filter [3 3]	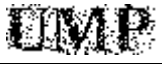	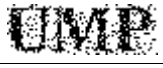	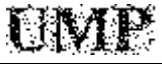	
Speckle noise 0.01				
Poisson noise				
Sharpening				
Cropping 25%				

Figure 8 Visual quality comparison of the extracted watermarks for the "Baboon" image under different types of attacks.

Table 1 PSNR performance under different threshold values.

Threshold	Baboon	Pepper	Boat	Airplane	Lena
1	44.912	44.894	44.898	44.895	44.922
0.75	47.411	47.393	47.397	47.394	47.421
0.5	50.932	50.915	50.919	50.916	50.943
0.25	56.953	56.935	56.939	56.936	56.963

Table 2 Full Error performance under different threshold values.

Threshold	Baboon	Pepper	Boat	Airplane	Lena
1	0.673	0.679	0.687	0.676	0.670
0.75	0.505	0.509	0.515	0.507	0.503
0.5	0.337	0.340	0.343	0.338	0.335
0.25	0.169	0.171	0.172	0.169	0.168

Table 3 NC after different types of attacks on Watermarked Image under different threshold values.

Attacks	T = 0.25		T = 0.5		T = 0.75		T = 1	
	Baboon	Pepper	Baboon	Pepper	Baboon	Pepper	Baboon	Pepper
No attack	1.000	1.000	1.000	1.000	1.000	1.000	1.000	1.000
JPEG compression Q = 10	0.609	0.584	0.607	0.568	0.604	0.577	0.601	0.586
JPEG compression Q = 30	0.792	0.660	0.802	0.687	0.822	0.777	0.851	0.859
JPEG compression Q = 50	0.846	0.753	0.867	0.809	0.904	0.914	0.923	0.961
JPEG compression Q = 70	0.901	0.825	0.923	0.902	0.953	0.957	0.957	0.981
JPEG compression Q = 90	0.972	0.952	0.977	0.975	0.986	0.991	0.989	0.996
Gaussian low pass filter [3 3]	0.927	0.913	0.928	0.925	0.932	0.949	0.939	0.966
Gaussian noise 0.01	0.813	0.727	0.825	0.763	0.847	0.832	0.877	0.874
Salt and pepper noise 0.05	0.799	0.718	0.820	0.748	0.850	0.794	0.862	0.827
Median filter [3 3]	0.891	0.892	0.889	0.890	0.906	0.921	0.912	0.944
Speckle noise 0.01	0.875	0.821	0.890	0.860	0.913	0.924	0.924	0.949
Poisson noise	0.900	0.837	0.923	0.881	0.929	0.948	0.935	0.966
Sharpening	0.980	0.971	0.981	0.977	0.984	0.988	0.992	0.991
Cropping 25%	0.939	0.894	0.939	0.895	0.940	0.896	0.940	0.897

From Tables 1 and 2, it can be seen that the threshold used for embedding the watermark has a significant effect on the imperceptibility of the watermark. A larger threshold makes the embedded watermark more robust while it results in a lower quality of the watermarked image. Table 3 shows the NC comparison of the watermarked image under different threshold values. The watermarked image underwent different types of attacks. The experimental results indicate

that the proposed scheme has a great resistance to format-compression attack: JPEG compression; denoising attacks: median filter, Gaussian low pass filter; noise attacks: Gaussian noise, salt and pepper noise, Poisson noise, speckle noise; image processing attacks: sharpening; geometrical attacks: cropping. This embedding watermark scheme provides perceptual invisibility to the human visual system and robustness against attacks. Embedding the watermark in deep-hole locations of the JPEG quantization tables makes it resistant against JPEG quantization tables in image compression and its location does not have a significant impact on the quality of the image reconstruction.

6 Conclusions

Digital image watermarking is useful for preventing unauthorized duplication of digital images. This research investigated watermark embedding in the lowest DCT psychovisual threshold based on entropy and edge entropy. The DCT psychovisual threshold indicates loopholes $C_{5,1}$, $C_{4,2}$, $C_{3,3}$ luminance and $C_{3,2}$, $C_{2,2}$, $C_{2,3}$ chrominance in the JPEG quantization tables, respectively. Embedding a watermark image in those loopholes of the JPEG quantization tables provides great resistance against JPEG compression. The proposed embedding watermark scheme was tested under different types of attacks. The experimental results showed that the watermarked images had high imperceptibility and the watermark recovery was robust against different types of attacks.

Acknowledgments

The authors would like to express very special thanks to Universiti Malaysia Pahang, Malaysia for providing financial support of this research project by UMP Research Grant Scheme (RDU160364).

References

[1] Halder, R., Pal, S. & Cortesi, A., *Watermarking Techniques for Relational Databases: Survey, Classification and Comparison*, Journal of Universal Computer Science, **16**(21), pp. 3164-3190, 2010.

[2] Cui, L. & Li, W., *Adaptive Multiwavelet-Based Watermarking through JPW Masking*, IEEE Transactions on Image Processing, **20**(4), pp. 1047-1060, 2011.

[3] Yang, Y., Sun, X., Yang, H., Lie, C.T. & Xiao, R., *A Contrast-Sensitive Reversible Visible Image Watermarking Technique*, IEEE Transactions on Circuit and Systems for Video Technology, **19**(5), pp. 656-667, 2009.

[4] Niu, Y., Kyan, M., Krishnan, S. & Zhang, Q., *A Combined Just Noticeable Distortion Model-Guided Image Watermarking*, Signal, Image and Video Processing, **5**(4), pp. 517-526, 2011.

[5] Parthasarathy A.K. & Kak, S., *An Improved Method of Content Based Image Watermarking*, IEEE Transactions on Broadcasting, **53**(2), pp. 468-479, 2007.
[6] Barni, M., Bartolini, F. & Piva, A., *Multichannel Watermarking of Color Images*, IEEE Transactions on Circuits and Systems for Video Technology, **12**(3), pp. 142-156, 2012.
[7] Tsui, T.K., Zhang, X.P. & Androutsos, D., *Color image watermarking using Multidimensional Fourier Transforms*. IEEE Transactions on Information Forensics and Security, **3**(1), pp. 016-028, 2008.
[8] Lu, C.S., Huang, S.K., Sze, C.J. & Liao, H.Y.M., *Cocktail Watermarking for Digital Image Protection*, IEEE Transactions on Multimedia, **2**(4), pp. 209-224, 2000.
[9] Kutter, M. & Wingkler, S., *A Vision-Based Masking Model for Spread Spectrum Image Watermarking*, IEEE Transactions on Image Processing, **11**(1), pp. 016-025, 2002.
[10] Wei, Z. & Ngan, K.N., *Spatio-Temporal Just Noticeable Distortion Profile for Grey Scale Image/Video in DCT Domain*, IEEE Transactions on Circuits and Systems for Video Technology, **19**(3), pp. 337-346, 2009.
[11] Lu, C.S. & Liao, H.Y.M., *Multipurpose Watermarking for Image Authentication and Protection*, IEEE Transactions on Image Processing, **10**(10), pp. 1579-1592, 2001.
[12] Abu, N.A., Ernawan, F., Suryana, N. & Sahib, S., *Image Watermarking Using Psychovisual Threshold over the Edge*, Information and Communication Technology, **7804**, pp. 519-527, 2013.
[13] Maity, S.P. & Kundu, M.K., *DHT Domain Digital Watermarking with Low Loss in Image Informations*. International Journal of Electronics and Communications, **64**(3), pp. 243-257, 2010.
[14] Abu, N.A. & Ernawan, F., *A Novel Psychovisual Threshold on Large DCT for Image Compression*, The Scientific World Journal, pp. 001-011, 2015.
[15] Ernawan, F. & Nugraini, S.H., *The Optimal Quantization Matrices for JPEG Image Compression From Psychovisual Threshold*. Journal of Theoretical and Applied Information Technology, **70**(3), pp. 566-572, 2014.
[16] Abu, N.A. & Ernawan, F., *Psychovisual Threshold on Large Tchebichef Moment for Image Compression*, Applied Mathematical Sciences, **8**(140), pp. 6951-6961, 2014.
[17] Ernawan, F., Abu, N.A., & Suryana, N., *An Optimal Tchebichef Moment Quantization Using Psychovisual Threshold for Image Compression*, Advanced Science Letters, **20**(1), pp. 70-74, 2014.
[18] Abu, N.A., Ernawan, F. & Sahib, S., *Psychovisual Model on Discrete Orthonormal Transform*, International Conference on Mathematical Sciences and Statistics, Kuala Lumpur, Malaysia, pp. 309-314, 2013.

[19] Abu, N.A., Ernawan, F. & Suryana, N., *A Generic Psychovisual Error Threshold for the Quantization Table Generation on JPEG Image Compression*, 9th International Colloquium on Signal Processing and its Applications, Kuala Lumpur, Malaysia, pp. 39-43, 2013.

[20] Ernawan, F., Abu, N.A. & Suryana, N., *Adaptive Tchebichef Moment Transform Image Compression Using Psychovisual Model*, Journal of Computer Science, **9**(6), pp. 716-725, 2013.

[21] Ernawan, F., Abu, N.A. & Suryana, N., *An Adaptive JPEG Image Compression Using Psychovisual Model*, Advanced Science Letters, **20**(1), pp. 26-31, 2014.

[22] Rodriguez-Sanchez, R., Martinez-Baena, J., Garrido, A., Garcia, J.A., Fdez-Valdivia, J. & Aranda, M.C., *Computer Vision Group*, University of Granada, [2014-03-20], http://decsai.ugr.es/cvg/dbimagenes/c512.php.

[23] Fridrich, J., Goljan, M., Du, R., Lossless Data Embedding for All Image Formats, in Security and Watermarking of Multimedia Contents IV, Proceedings of SPIE, **4675**, pp. 572-583, 2002.

[24] Amer, I., Hishmat, P., Badawy W., Jullien, G., *Comparisons and Analysis of DCT-based Image Watermarking Algorithm*, Advanced Techniques in Computing Sciences and Software Engineering, pp. 055-058, 2010.

[25] Khalighi, S. & Rabiee, H., *A Contourlet-based Image Watermarking Scheme with High Resistance to Removal and Geometrical Attacks*. EURASIP Journal on Advances in Signal Processing, **2010**, pp. 001-013, 2010.

[26] Yim, C. & Bovik, A.C., *Quality Assessment of Deblocked Images*, IEEE Transactions on Image Processing, **20**(1), pp. 088-098, 2011.

[27] Wang, Z., Bovik, A.C., Sheikh, H.R. & Simoncelli, E.P., *Image Quality Assessment: From Error Visibility to Structural Similarity*, IEEE Transactions on Image Processing, **13**(4), pp. 600-612, 2004.

[28] You, X., Du, L., Cheung, Y. & Chen, Q., *A Blind Watermarking Scheme Using New Nontensor Product Wavelet Filter Banks*, IEEE Transactions on Image Processing, **19**(12), pp. 3271-3284, 2010.